



## Developing Wearable Robot that Mimics Natural Walking Mechanism to Support Children with Cerebral Palsy in their Lower Limbs

Mariam Muhammad Al-Abasi\* and Abdusalam Imhmed K. AlKhwaji

Department of Mechanical and Industrial Engineering, Faculty of Engineering, Alasmarya Islamic University,  
Zliten, Libya.

\*المبريد الإلكتروني: mariamalabasi43@gmail.com

### تطوير روبوت قابل للارتداء يحاكي آلية المشي الطبيعية لدعم الأطفال المصابين بالشلل الدماغي في أطرافهم السفلية

مريم محمد العباسي\* وعبد السلام امحمد القهواجي

قسم الهندسة الميكانيكية والصناعية، كلية الهندسة، الجامعة الأسمرية الإسلامية، زلiten، ليبيا

#### Abstract

A pioneering "Crank-Rocker" mechanism was developed in industrial biomechanics to simulate natural walking in a wearable robot. The project aims to assist children with lower limb motor impairments and reduce the robot's cost by minimizing the number of motors. An 8-year-old child model, weighing 16 kg and measuring 116 cm in height, suffering from lower limb motor impairment, was selected. The mechanism was designed using rigid elements inspired by the human leg's anatomy (bones and muscles) to simulate the muscular systems in wearable robots. The condition causes muscle atrophy, affecting bone movement and range of motion control. The mechanism consists of two main parts: the driving part, powered by a DC motor, which represents the Crank-Rocker mechanism, and the dependent part, representing the human leg. The mechanism was transformed into a multi-arm system, reducing the number of motors per foot to a single motor. A motor with a movable shaft structure was incorporated, connecting both feet with a single motor to ensure instantaneous synchronization of their movement. This also contributed to simplifying the control system and reducing the economic cost. The movement of the mechanism was simulated using SolidWorks, and a mathematical model for motion analysis was created using the closed-loop method. Additionally, Kinova software was used to analyze the movement and compare it with that of a healthy child. The results showed that the mechanism achieves a similar motion pattern to the natural walking of healthy children within GMFCS levels III and IV, enhancing

the effectiveness of the mechanism in closely replicating a natural walking pattern. This project aims to assist children with lower limb motor impairments and reduce the robot's cost by minimizing the number of motors, thereby improving their quality of life.

**Keywords:** Biomechanics, Crank-Rocker mechanism, Wearable robot, Cerebral palsy, KINOVA

### الملخص

تم تطوير آلية "Crank-Rocker" الميكانيكية في مجال الميكانيكا الصناعية الحيوية، بهدف محاكاة المشي الطبيعي للأطفال ذوي الإعاقات الحركية في الأطراف السفلية. تم اختيار نموذج لطفل يبلغ من العمر 8 سنوات، وزنه 16 كجم وطوله 116 سم، يعاني من ضعف حركي في الأطراف السفلية. تتكون الآلية من جزئين رئيسيين: الجزء المحرك الذي يعمل بواسطة محرك تيار مستمر، والجزء التابع الذي يمثل الساق البشرية. تم تحويل الآلية إلى نظام متعدد الأذرع، مما يقلل عدد المحركات إلى محرك واحد لكل قدم. تم دمج محرك بهيكل عمود دوار، يربط بين القدمين بمحرك واحد لضمان التزامن الفوري لحركتهما، مما يبسط النظام التحكم ويقلل التكلفة الاقتصادية. تم محاكاة حركة الآلية باستخدام برنامج SolidWorks، وتم إنشاء نموذج رياضي لتحليل الحركة باستخدام طريقة الحلقة المغلقة. بالإضافة إلى ذلك، تم استخدام برنامج Kinova لتحليل الحركة ومقارنتها بحركة طفل سليم. أظهرت النتائج أن الآلية تحقق نمط حركة مشابهًا للمشي الطبيعي للأطفال الأصحاء ضمن مستويات GMFCS III و IV، مما يعزز فعالية الآلية في محاكاة نمط المشي الطبيعي. يهدف هذا المشروع إلى مساعدة الأطفال ذوي الإعاقات الحركية في الأطراف السفلية، وتقليل تكلفة الروبوت من خلال تقليل عدد المحركات، مما يسهم في تحسين جودة حياتهم.

الكلمات الدالة: البيوميكانيك، آلية كرنك روكر، روبوت قابل للارتداء، الشلل الدماغي، كينوفا.

## 1. Introduction

Cerebral palsy is considered the most common movement disorder among children, resulting from brain damage that occurs either before birth or during the early years of life. Children with this condition face walking difficulties due to irregular gait patterns, involuntary muscle contractions, and spasms, which negatively impact their independence and quality of life, while increasing their energy consumption during walking. Although cerebral palsy is regarded as an incurable disorder, my study has focused on designing wearable robots to support the lower limbs, aiming to improve walking efficiency for affected children, reduce energy consumption, and enhance their independence and social interaction (Molnar, 1991).

Wearable robots are biomechatronic devices that mimic the structure and function of human limbs, representing a union between two fields: the medical field, which involves the study of the human leg in terms of bones, muscles, ligaments, and nerves, and the engineering field, which aims to develop a mechanism that mimics the human leg's structure and provides movement similar to human walking, along with appropriate motors and sensors that simulate human nerves. When used as a treatment for children with cerebral palsy, these devices act as assistive devices to compensate for the lack of motor functions and reduce energy consumption during walking. They also help resist the effects of gravity, which reduces the effort required



from the muscles to move the limbs. Thus, these devices offer a suitable solution to provide children with the opportunity to live their lives more naturally (Pons, 2008).

The types of these robots vary depending on the disability they aim to treat. Among the most notable are multi-joint wearable robots, such as the "WAKE-up" device, which restores natural walking patterns by supporting the ankle and knee joints, as well as other devices like "Atlas2030" and "Trexo". These robots provide stability through weight distribution, but some designs may impact flexibility and limit the development of balance skills. The studies that these devices rely on use simple mechanisms, with the use of brushed DC motors for each of the three joints, requiring precise control systems like the PID system. However, the high cost of these motors makes them difficult for many families to afford, presenting a challenge in making them widely accessible (Pons, 2008).

This research aims to develop a "crank-rocker" mechanism for a wearable robot designed to treat children with cerebral palsy, aiming to improve their quality of life while reducing the robot's cost by minimizing the number of motors used in traditional designs, making it accessible to a wider range of families. The mechanism converts rotational motion into oscillatory motion, focusing on representing the muscles affected by atrophy caused by the condition. The mechanism was designed using SolidWorks software, and its motion was simulated to verify its efficiency. It relies on two interconnected systems: the leading system, which simulates the muscles supporting the pelvis and femur, and the driven system, which mimics the human leg's structure, including bones, muscles, and ligaments. Finally, the resulting motion was compared to that of a healthy child using the "Kinova" motion analysis program to ensure the design's efficiency.

## **2. Patients, Material, and Methods**

Developing a wearable robot for the lower limb is a complex process that requires comprehensive integration of medical information related to gait mechanisms and human leg anatomy, along with the design of a mechanical system capable of generating the required motion to simulate natural walking patterns. This system aims to synchronize with the movement of the mechanism representing the human leg.

### **2.1. Patients**

In this section, a case study is presented focusing on addressing cerebral palsy in children. A child aged 8 years, weighing 16 kg and measuring 116 cm in height, was diagnosed with bilateral cerebral palsy at the age of 6 at Zliten Medical Center in 2021. An analysis of human leg anatomy, including muscles and bones, was conducted to understand the condition. The two primary phases of gait, the "stance" and "swing" phases, were also examined. The objective is to assist the child in movement according to GMFCS levels III and IV (Molnar, 1991; Collins & De Luca, 1993; Ko et al., 2001; and Pons, 2008), as shown in Figure (1).

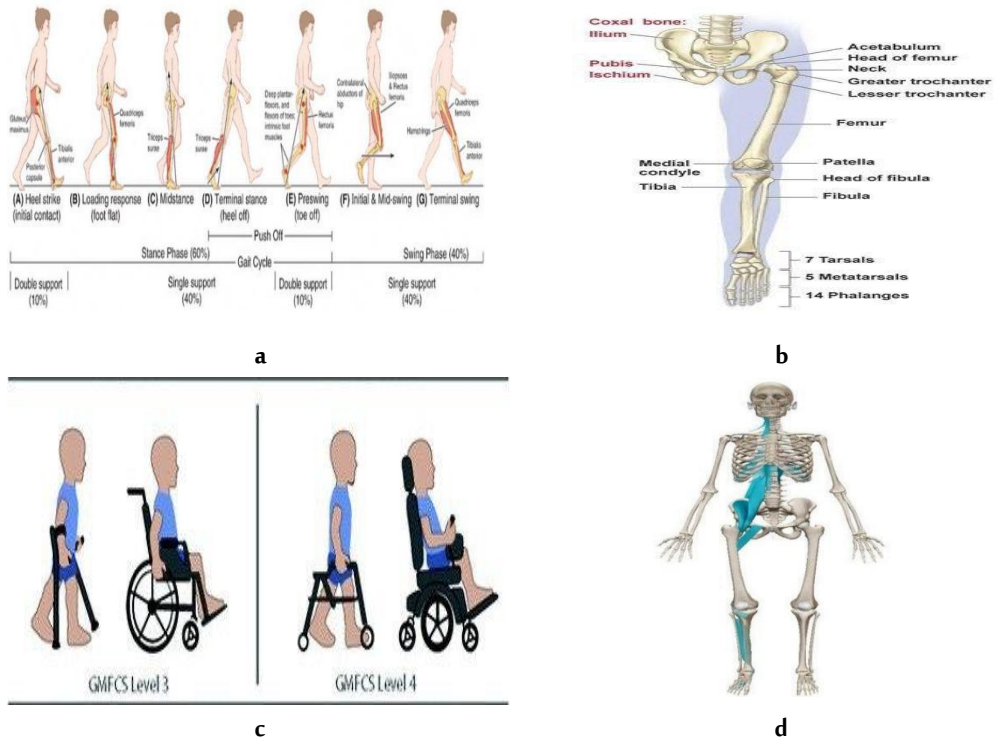


Figure 1. a) the walking mechanism, b) the structure of the leg including bones and joints, c) as well as specifying the required motion levels for the mechanism to enable it, d) the part that the lateral muscles should mimic on the lateral side"

## 2.2. Material

In this section, the culprit represents the materials used to develop a prototype mechanism represented by the following points:

### Development of a Wearable Robot Using the "Crank -Rocker" Mechanism

Based on the mechanism adopted for developing the wearable robot, the "Crank-Rocker" mechanism was selected. This mechanism was divided into a leader part and a follower part.

### Influence of the Mechanism on the Leader Part

In the driven mechanism, the crank-rocker mechanism, operated by a DC motor to change the direction of the crank movement, was geometrically represented to reflect the design of the essential lateral muscles represented by elements. Since there are two elements, two crank-rocker mechanisms were obtained for the mechanism as shown in Figure (2.c).

Additionally, one element was represented in the shape of the 'I' and the other in the shape of the 'L' to achieve the maximum distance, which occurs when points 1 and 2 align on a straight line, as illustrated in Figure (2.a).

### Driven Mechanism for Simulating Human Leg Biomechanics

The driven mechanism represents the human leg, including the bones, muscles, and joints, as shown in Figure (2.b). The driving mechanism provides the initial rotational motion, which is converted into linear reciprocating motion, enabling accurate simulation of the natural movement of the human leg.

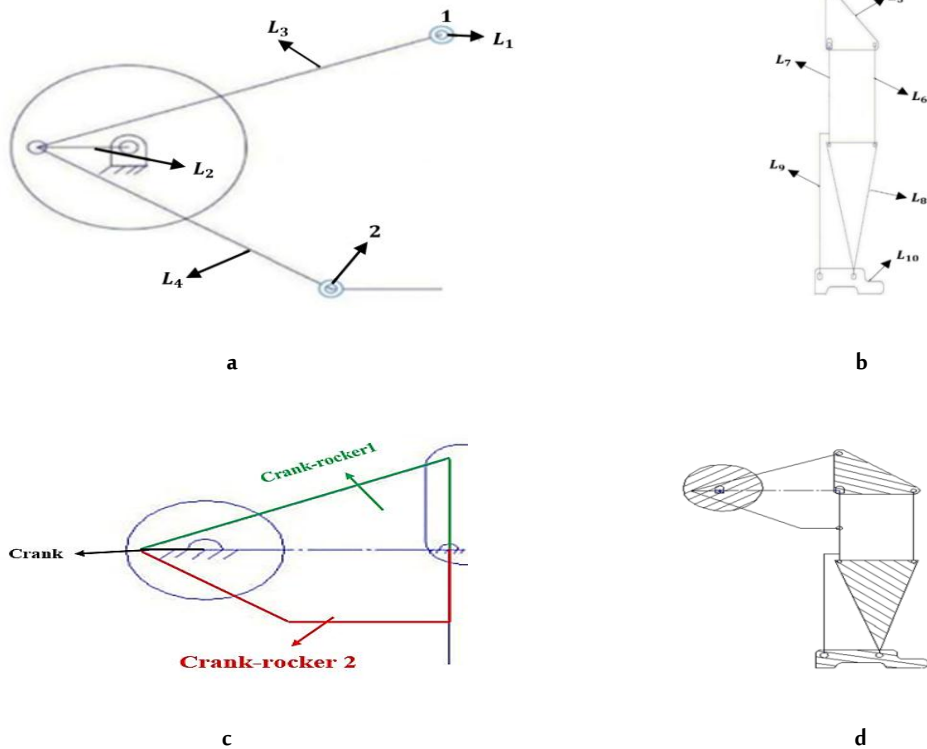


Figure 2. The following; a) The driving mechanism, b) The driven mechanism, c) Rocker crank mechanism in mechanics, and d) Model mechanism.

Table (1) illustrates all the components of both the driven and driving mechanisms, as shown in Figure (2.d), and their roles in simulating the biomechanics of the human leg. It is worth noting that all elements were represented using rigid components of two types:

- Rigid Link "Binary"
- Rigid Link "Ternary"



The binary link connects two links, while the ternary link connects three links. These links are used in the design of mechanisms to achieve the desired motion, such as simulating the movement of the human leg.

**Table1. Illustrates each component and its corresponding counterpart in the human leg, as well as the connection points of the components, representing joints or muscle attachments.**

The Link	TypeLink	Interpretation of each element in the mechanism	Length unit	Explains all the details of the joints in the mechanism	Joint type
<b>L<sub>1</sub></b>	Fixed linke	Ligament (iliofemoral, pubofemoral, ischiofemoral). Communication from the drive system.	mm	It represents the point of contact with the crank, and point C corresponds to the pelvic bone, which represents Ligament of the hip joint	Rotational (Binary)
<b>L<sub>2</sub></b>	Rigid Link "Binary"	"Crank"	mm	//	Rotational (Ternary)
<b>L<sub>3</sub></b>	Rigid Link "Binary"	Lateral muscles (gulte medius)	mm	It represents the point of contact of the gulte medius muscle group with the pelvic bone	Rotational (Binary)
<b>L<sub>4</sub></b>	Rigid Link "Binary"	Lateral muscles (gulte maximus)	mm	It represents the point of contact of the gulte maximus muscle group with the femur bone	Rotational (Binary)
<b>L<sub>5</sub></b>	Rigid Link "Ternary"	the hip joint	mm	Represents the hip joint	Rotatinal (Ternary)
<b>L<sub>6</sub></b>	Rigid Link "Binary"	Represents the femur bones	mm	With L8The posterior connection of the knee joint to the femur	Rotatinal (Binary)
<b>L<sub>7</sub></b>	Rigid Link "Binary"	Represents the patellae bones	mm	With L8The anterior connection of the knee joint to the femur	Rotatinal (Binary)
<b>L<sub>8</sub></b>	Rigid Link "Ternary"	Represents the tibia bones	mm	With L10 connected to the middle foot of the ankle joint	Rotatinal (Binary)
<b>L<sub>9</sub></b>	Rigid Link "Binary"	Represents the fibula bones	mm	With L10 connected to the back foot of the ankle joint	Rotatinal (Binary)
<b>L<sub>10</sub></b>	Rigid Link	Represents the foot	mm	The foot	//

To test the required smoothness of the movement, A.W. Klein was used according to Eqn. (1), where the system includes l elements, j double pairs, and h super pairs. In addition, the degrees of freedom required for

*Developing Wearable Robot that Mimics Natural Walking Mechanism.....*

movement were calculated using the Kutzbach criterion according to Eqn. (2), specifying the values required to achieve optimal movement at (x, y) (Khurmi & Gupta, 2005; and Uicker et al., 2023).

$$j + \frac{h}{2} = \frac{3}{2}l - 2 \quad \dots\dots (1)$$

$$n = 3(l - 1) - 2j - h \quad \dots\dots (2)$$

To represent the mechanism, the lengths of the selected case's bones (femur and tibia) were measured according to the method adopted by the Misrata Prosthetics Center, following the instructions of the responsible doctor during the visit for fabricating the prosthetic mold. This method includes adding 2 cm to the bone length to compensate for the coupling at the ends of the element. The measurements were recorded in centimeters (cm), and a scale of 1 cm:1 mm was applied in SolidWorks for representation. The joints were depicted in a circular shape, considering their radius, as illustrated in Figure (3.a). The model was then assembled in SolidWorks, as shown in Figure (3.b).

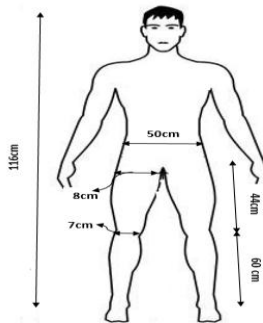


Figure 3.a. The bone dimensions of the child used as a case study

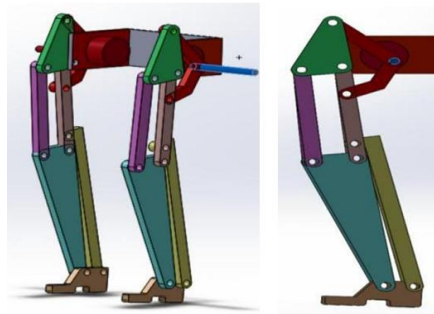
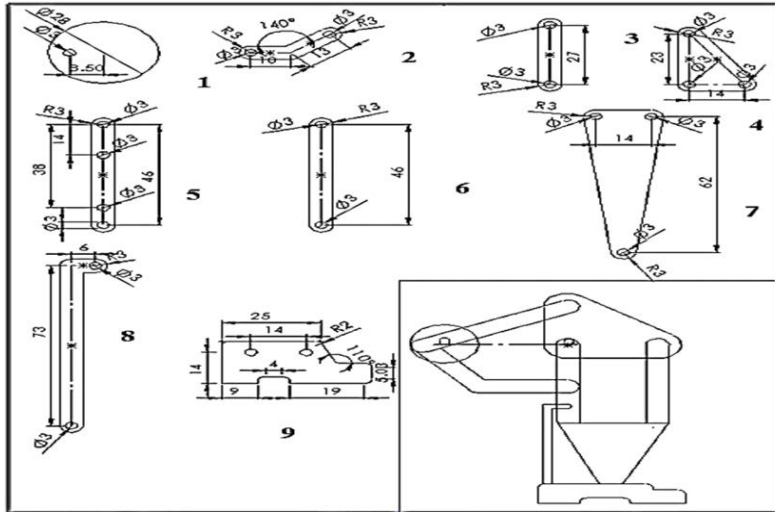


Figure 3.b. The representation of the mechanism elements and their assembly using SolidWorks

After the model was simulated and assembled using SolidWorks, a physical prototype was created using a 4mm-thick Kobax material, as shown in Figure (4).



Figure 4. Actual model made with Kobax



*Developing Wearable Robot that Mimics Natural Walking Mechanism.....*

Determining the position and direction of each component and joint in wearable robots is essential for safely and efficiently achieving therapeutic goals. Using a multi-arm mechanism composed of rigid components and rotational joints, the loop closure equations (connection matrices) method was employed to ensure precise positioning. The mechanism was divided into four closed loops, beginning with the driving mechanism (crank-rocker) and ending with the last component, the foot, as illustrated in Figure (5). All analyses were conducted using the Complex form method as described in Eqn. (3), where represents  $R_i^{\rightarrow}$  the position and direction vector for each component,  $r_i$  the length of each component, and  $e^{i\theta}$  the Complex form direction component (Collins & De Luca, 1993; Khurmi & Gupta, 2005; and Uicker et al., 2023).

$$(R_i^{\rightarrow})_{input} = (R_i^{\rightarrow})_{output} \quad \dots\dots (3)$$

Where,  $R_i^{\rightarrow} = r_i e^{i\theta}$

$$e^{i\theta} = (\cos \theta_i + i \sin \theta_i)$$

The ground conduction element has a zero angle as it is fixed, while the crank element's angle varies from 0 to 360 degrees. Each element has two directions: a real direction (movement along x and y) and an imaginary direction (rotation around z), as shown in Eqns. (4) and (5);

$$\text{Real} \quad (L_i \cos \theta_i)_{input} = (L_i \cos \theta_i)_{output} \quad \dots\dots (4)$$

$$\text{Img} \quad (L_i i \sin \theta_i)_{input} = (L_i i \sin \theta_i)_{output} \quad \dots\dots (5)$$

To determine the position and orientation of each component of the mechanism, each closed loop was analyzed as follows:

**Loop1:**

From Eqn. (6), the closed-loop1, to find the position of element 3, from Eqn. (7).

$$R_1^{\rightarrow} + R_2^{\rightarrow} + R_3^{\rightarrow} = R_4^{\rightarrow} \quad \dots\dots (6)$$

$$2L_1(L_2 \cos \theta_2 + L_3 \cos \theta_3) + (L_2 \cos \theta_2 + L_3 \cos \theta_3)^2 + (L_2 \sin \theta_2 + L_3 \sin \theta_3)^2 = L_4^2 - L_1^2 \quad \dots\dots (7)$$

where

$$\cos \theta_3 = \frac{1 - (\tan \frac{\theta_3}{2})^2}{1 + (\tan \frac{\theta_3}{2})^2} \quad \sin \theta_3 = \frac{2 \tan \frac{\theta_3}{2}}{1 + (\tan \frac{\theta_3}{2})^2}$$

To determine the position of the fourth and final element in this loop, find it by substituting the position of the third element into the equation, whether it is the Real equation or the Img equation.

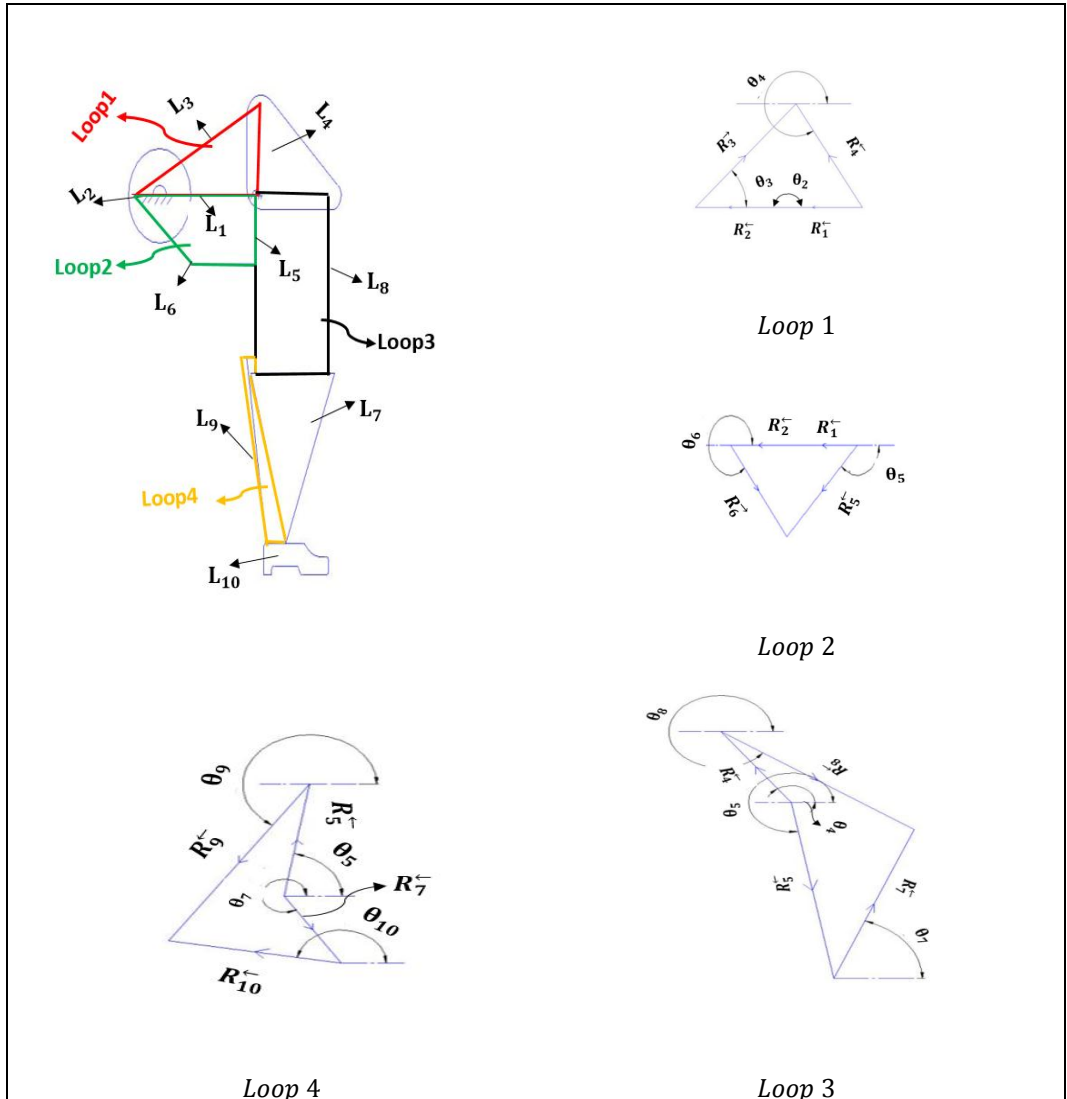


Figure 5. The division of the mechanism into four closed loops for geometric position analysis shows each component of the mechanism.

**Loop2:**

From Eqn. (8), the closed-loop2, to find the position of element 6, from Eqn. (9).

To determine the position of the fifth and final element in this loop, find it by substituting the position of the sixth element in the equation, whether it is the real equation or the  $\text{Im}g$  equation.



$$R_1^{\rightarrow} + R_2^{\rightarrow} + R_6^{\rightarrow} = R_5^{\rightarrow} \quad \dots (8)$$

$$2L_1L_6 \cos \theta_2 \cos \theta_6 + 2L_1L_6 \sin \theta_1 \sin \theta_6 + 2L_2 \cos \theta_2 (L_1 \cos \theta_1 + L_6 \cos \theta_6) + 2L_2 \sin \theta_2 (L_1 \sin \theta_1 + L_6 \sin \theta_6) = L_5^2 - L_1^2 - L_6^2 - L_2^2 \quad \dots (9)$$

Where  $\cos \theta_6 = \frac{1 - (\tan \frac{\theta_6}{2})^2}{1 + (\tan \frac{\theta_6}{2})^2}$   $\sin \theta_6 = \frac{2 \tan(\frac{\theta_6}{2})}{1 + (\tan \frac{\theta_6}{2})^2}$

**Loop3:**

From Eqn. (10), the closed-loop3, to find the position of element 7, from Eqn. (11).

$$R_4^{\rightarrow} + R_8^{\rightarrow} = R_5^{\rightarrow} + R_7^{\rightarrow} \quad \dots (10)$$

$$(L_5 \cos \theta_5 + L_7 \cos \theta_7)^2 + 2L_4 \cos \theta_4 (L_5 \cos \theta_5 + L_7 \cos \theta_7) + (L_5 \sin \theta_5 + L_7 \sin \theta_7)^2 + 2L_4 \sin \theta_4 (L_5 \sin \theta_5 + L_7 \sin \theta_7) = L_8^2 + L_4^2 (\cos \theta_4)^2 + L_4^2 (\sin \theta_4)^2 \quad \dots (11)$$

Where:  $\cos \theta_7 = \frac{1 - (\tan \frac{\theta_7}{2})^2}{1 + (\tan \frac{\theta_7}{2})^2}$   $\sin \theta_7 = \frac{2 \tan(\frac{\theta_7}{2})}{1 + (\tan \frac{\theta_7}{2})^2}$

To determine the position of the eighth and final element in this loop, find it by substituting the position of the seventh element in the equation, whether it is the real equation or the lmg equation.

**Loop4:**

From Eqn. (12), the closed-loop4, to find the position of element 9, from Eqn. (13).

$$R_5^{\rightarrow} + R_9^{\rightarrow} = R_7^{\rightarrow} + R_{10}^{\rightarrow} \quad \dots (12)$$

$$2L_9^2 (\sin \theta_9)^2 (L_5 \sin \theta_5 - L_7 \sin \theta_7)^2 + 2L_9^2 (\cos \theta_9)^2 (L_5 \cos \theta_5 - L_7 \cos \theta_7)^2 = L_{10}^2 - L_5^2 - L_7^2 - L_9^2 - L_5L_7 \cos \theta_7 \sin \theta_5 - L_5L_7 \cos \theta_5 \sin \theta_7 \quad \dots (13)$$

Where:  $\cos \theta_9 = \frac{1 - (\tan \frac{\theta_9}{2})^2}{1 + (\tan \frac{\theta_9}{2})^2}$   $\sin \theta_9 = \frac{2 \tan(\frac{\theta_9}{2})}{1 + (\tan \frac{\theta_9}{2})^2}$

To determine the position of the tenth and final element in this loop, find it by substituting the position of the ninth element in the equation, whether it is the real equation or the lmg equation.

**2.3. Methods**

A multi-arm wearable robot mechanism for the lower limbs was developed using the "Crank-Rocker" mechanism to simulate human leg movement. The leg structure and gait mechanism were analyzed to determine the required movement levels for enabling a child with cerebral palsy. Kinematic analysis was performed using the Kutzbach criteria to determine the degrees of freedom. A geometric model was designed in SolidWorks to simulate movement, and the positions of the components were analyzed using loop closure equations to ensure motion accuracy and efficiency.

### 3. Results & Discussion

A healthy child with physical characteristics similar to the affected child was selected, and a computational model was created using SolidWorks to simulate the movement of the affected child's leg. The movement of both the healthy child and the simulated model was recorded to perform a kinematic analysis of the knee and ankle joint positions over 38 points representing a complete gait cycle, from the initiation of movement to its conclusion by using "KINOVA" (Yusof et al., 2022) as show Figures (6 & 7).

This type of kinematic analysis is used to understand the dynamics of movement and to identify the differences between the natural and simulated movements of the prepared model after the model has proven its effectiveness in reducing the number of motors as proven by Eqn. (2) to prove the efficiency of the model.

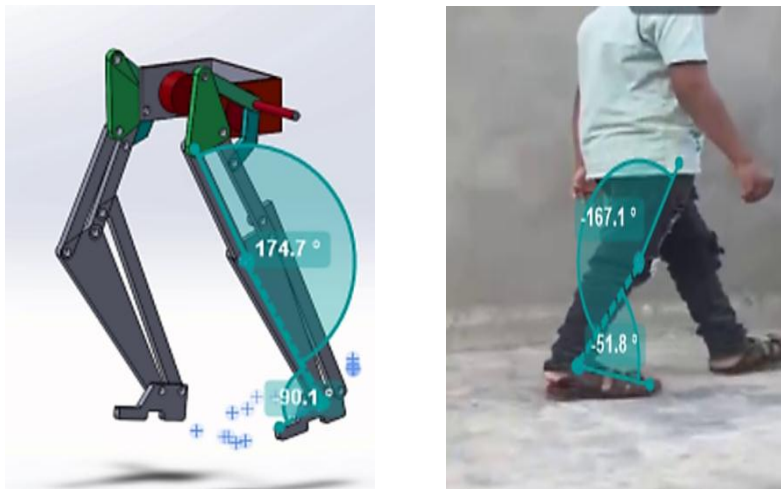
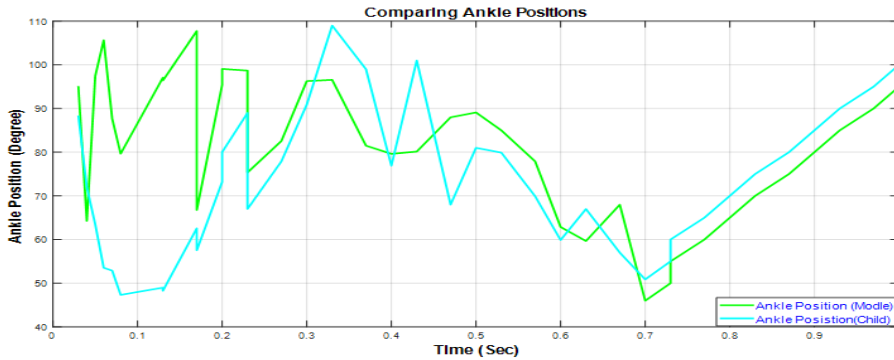
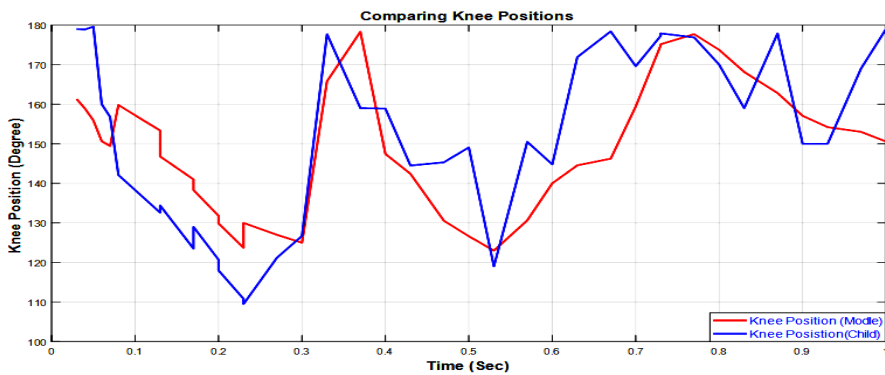


Figure 6. Kinetic analysis of Kenova



a



b

Figure 7. Comparison of the results of kinematic analysis of the plasma joint and the composite model and natural motion

#### 4. Conclusion

The study used a crank-lever mechanism to simulate the mechanical relationship between muscles and bones in the human leg during walking, reducing the need for multiple motors to just one. A simulation model was developed using SolidWorks. A low-cost physical prototype was manufactured using Kobax. A mathematical model was derived and the motion of the knee and ankle joints was analyzed. Despite some challenges in applying mathematical modeling to IMU sensors, the results demonstrated the effectiveness of the methodology and its potential for



## References

- Collins, J. J., & De Luca, C. J. (1993). Open-loop and closed-loop control of posture: a random-walk analysis of center-of-pressure trajectories. *Experimental brain research*, 95, 308-318.
- Guzmán-Valdivia, C. H., Blanco-Ortega, A., Oliver-Salazar, M. A., & Carrera-Escobedo, J. L. (2013). Therapeutic motion analysis of lower limbs using Kinovea. *Int J Soft Comput Eng*, 3(2), 2231-307.
- Khurmi, R. S. & Gupta, J.K. (2005). *Theory of Machines*, 14<sup>th</sup> ed. Chand & Co. Ltd., New Dehli.
- Ko, J., Woo, J. H., & Her, J. G. (2011). The reliability and concurrent validity of the GMFCS for children with cerebral palsy. *Journal of physical therapy science*, 23(2), 255-258.
- Molnar, G. E. (1991). Rehabilitation in cerebral palsy. *Western journal of medicine*, 154(5), 569.
- Pons, J. L. (2008). *Wearable robots: biomechatronic exoskeletons*. John Wiley & Sons.
- Uicker, J. J., Uicker Jr, J. J., Pennock, G. R., & Shigley, J. E. (2023). *Theory of machines and mechanisms*. Cambridge University Press..
- Yusof, Y. A., Hisham, N. A. H., Ab Patar, M. N. A., Le, C. H., Mahmud, J., Lee, H., Yamamoto, S., & Herawati, L. (2022, July). Walking gait analysis: kinovea versus motion capture system. In: *2022 IEEE 13<sup>th</sup> Control and System Graduate Research Colloquium (ICSGRC)* (pp. 187-191). IEEE.